ORIGINAL RESEARCH

Apoptotic induction and inhibition of NF-κB signaling pathway in human prostatic cancer PC3 cells by natural compound 2,2′-oxybis (4-allyl-1-methoxybenzene), biseugenol B, from *Litsea costalis*: an in vitro study

Maryam Abbaspour Babaei[1]
Hasniza Zaman Huri[1,2]
Behnam Kamalidehghan[3,4]
Swee Keong Yeap[5,6]
Fatemeh Ahmadipour[1]

[1]Department of Pharmacy, Faculty of Medicine, University of Malaya, Kuala Lumpur, Malaysia; [2]Clinical Investigation Centre (CIC), University of Malaya Medical Centre, Kuala Lumpur, Malaysia; [3]Medical Genetics Department, School of Medicine, Shahid Beheshti University of Medical Sciences, Tehran, Iran; [4]Medical Genetics Department, National Institute for Genetics Engineering and Biotechnology (NIGEB), Tehran, Iran; [5]Institute of Bioscience, Universiti Putra Malaysia, Serdang, Malaysia; [6]Xiamen University Malaysia, Sepang, Malaysia

Correspondence: Hasniza Zaman Huri; Maryam Abbaspour Babaei
Department of Pharmacy, Faculty of Medicine, Level 3, Block R., University of Malaya, Jalan Universiti, 50603 Kuala Lumpur, Wilayah Persekutuan Kuala Lumpur, Malaysia
Email hasnizazh@um.edu.my; maryammab@gmail.com

Abstract: *Litsea* is considered as an evergreen genus distributed in tropical and subtropical Asia; this genus belongs to the large family of Lauraceae. In this study, the cell-death metabolism of biseugenol B was investigated. Nuclear condensation, cell permeability, mitochondrial membrane potential (MMP) and release of cytochrome c have been detected in human prostate cancer cell line (PC3) treated with biseugenol B by high content screening (HCS). Fluorescent analysis was conducted to examine the reactive oxygen species formation. To determine the mechanism of cell death, the levels of Bcl-cell lymphoma (Bcl)-2 proteins, Bcl-2-associated X (Bax) protein and anti-apoptosis heat-shock protein 70 were tested by applying reverse transcription polymerase chain reaction and Western blot. Bioluminescent assays were also performed to assess the level of caspases such as 3/7, 8 and 9 during treatment. Furthermore, the involvement of nuclear factor kappa-B (NF-κB) was examined by Western blot and HCS. Biseugenol B showed significant cytotoxicity toward PC3 with no toxicity toward normal prostate cells (RWPE-1), which indicates that biseugenol B has qualities that induce apoptosis in tumor cells. The treatment of PC3 cells with biseugenol B provoked apoptosis with cell-death-transducing signals. Downregulation of Bcl-2 and upregulation of Bax regulated the MMP, which in turn caused the release of cytochrome c from mitochondria into cytosol. The release of cytochrome c activated caspase-9, which consequently activated caspase-3/7 with the cleaved poly(ADP-ribose) polymerase protein, thereby resulting in apoptosis alteration. Involvement of an extrinsic apoptosis pathway was exhibited by the increase in caspase-8, while the increase in caspase-3/7 and caspase-9 demonstrated involvement of an intrinsic apoptosis pathway. Meanwhile, no significant increase was observed in caspases 3/7, 8 or 9 in normal prostate cells (RWPE-1) after treatment with biseugenol B. Prevention of NF-κB translocation from the cytosol to the nucleus occurred in PC3 after treatment with biseugenol B. The results of our study reveal that biseugenol B triggers the apoptosis of PC3 cells via intrinsic and extrinsic apoptosis pathways and inhibition of NF-κB signaling pathway. Our findings suggest that biseugenol B is a potentially useful agent for prostate cancer treatment.

Keywords: biseugenol B, apoptosis, mitochondria, caspase, intrinsic, extrinsic, NF-κB

Introduction

Prostate cancer or carcinoma of the prostate is the second most common type of cancer and the fifth leading cause of cancer-related death in men globally.[1] More than

277

1.1 million cases of prostate cancer were recorded in 2012, accounting for ~8% of all new cancer cases and 15% of all cancer cases in men.[2] In Malaysia, prostate cancer is the fourth most common type of cancer diagnosed in men.[3]

Conventional cancer therapy involves surgery, radiotherapy, chemotherapy and occasionally hormone and immune therapy. Radiation therapy has been a useful tool in cancer treatment since 1960 and is often used along with surgery. However, like surgery, radiotherapy alone cannot prevent metastatic cancer. Meanwhile, chemotherapy is based on applying certain drugs to retard or destroy the growth of malignant cells. The anti-tumor effect of most chemotherapy drugs is due to apoptosis or inducing growth arrest of cancer cells. However, the side effects of these drugs are significant and noticeable. The side effects often include damage in bone-marrow blood cells, digestive tract, hair follicles and mouth cells.[4] To avoid the major side effects of chemotherapy drugs, herbal medicine has been considered as an alternative cancer therapy because of its lower toxicity and cost benefits.[5] Natural products or herbs have been used around the world in clinical attempts to cure cancer.[6] In addition, the direct suppression effect of cancer cell proliferation has been reported as a result of using certain herbs and their constituents.[7] *Litsea costalis* is considered as an evergreen genus distributed in tropical and subtropical Asia, as well as in North and South America.[8] *Litsea* is used widely in People's Republic of China and Malaysia as a traditional medicine for influenza and stomachache.[9] In addition, *Litsea* contains neolignans, a chemical compound in plants, which is used in traditional Chinese medicine to treat viral hepatitis and to protect the liver.[10] Neolignans also exhibit pharmacological activity in mammalian cells.[11] Moreover, N6-isopentenyladenosine (iPA), isolated from *L. costalis*, regulates plant cell growth and differentiation.[12,13] A new compound, 2,2′-oxybis (4-allyl-1-methoxybenzene) or biseugenol B, has been isolated from *L. costalis* and belongs to the main group of natural origin, neolignan and oxyneolignan, which possess anti-proliferative and anti-cancer properties.[14–16] The chemical structure of 2,2′-oxybis (4-allyl-1-methoxybenzene) or biseugenol B is shown in Figure 1.[17]

In this study, we evaluated the apoptosis cell-death mechanism through a novel compound called biseugenol B using human prostate cancer cells (PC3) as an in vitro model.

Methodology
Cell culture
Prostate cancer cells (PC3) and normal prostate cells (RWPE-1)[18] were obtained from the American Type Cell
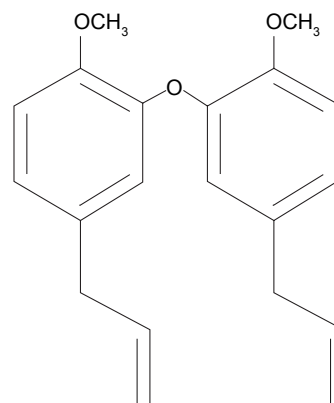

Figure 1 Structures of compound 2,2′-oxybis (4-allyl-1-methoxybenzene) or biseugenol B.

Collection (Manassas, VA, USA) and incubated at 37°C with 5% CO_2.[19] Prostate cancer cells (PC3) were cultured in Roswell Park Memorial Institute (RPMI)-1640 medium with 10% fetal bovine serum (FBS) and 1% of 100 unit/mL of penicillin and streptomycin,[20] and normal prostate cells (RWPE-1) were cultured in a concentration of 4×10^4 keratinocyte serum-free medium (K-SFM) supplemented with 0.2 ng/mL human epidermal growth factor (rhEGF) and 25 µg/mL bovine pituitary extract (BPE)[21] and 1× antibiotic/antimycotic solution. Cultures were incubated at 37°C in a humidified atmosphere containing 5% CO_2 and passed weekly.[22–24]

Cell viability assay (3-(4,5-dimethylthiazol-2-yl)-2,5-diphenyltetrazolium bromide (MTT))
By using MTT assay, viability assay was performed as described by Mohan.[19] Briefly, 5×10^4 cells were treated with biseugenol B at different concentrations in a 96-well plate and maintained in incubation for 24, 48 and 72 hours. At absorbance of 570 nm, the colorimetric assay was measured and recorded. The results were taken as a percentage of control giving percentage cell viability after 24, 48 and 72 hours exposure to test agent. The half maximal inhibitory concentration (IC_{50}) value was measured as the potency of cell growth inhibition for test agent.[19]

Quantification of apoptosis using propidium iodide (PI) and acridine orange (AO) double staining
The method of quantification of apoptosis was performed by applying AO and PI double staining. Cell death induced by biseugenol B in PC3 prostate cancer cells was measured based on the regular process as they were being observed under a fluorescence microscope (Lieca attached

with QFloro Software; Wetzlar, Germany).[19] Concisely, 2×10^5 of PC3 cells were treated with different concentrations of biseugenol B in a 25-mL culture flask (Techno Plastic Products AG; Trasadingen, Switzerland), which was performed before incubation of flasks in a humidity of 5% CO_2 at 37°C for 24 hours. Later, for 10 minutes, the cells were spun down at 1,800 rpm resulting in eliminating the supernatant, and the pellet was washed two times by using cold phosphate-buffered saline in order to eliminate the media. Then, the addition of 10 µL of mixed fluorescent dye PI (10 µg/mL) and AO (10 µg/mL) to the cellular pellet was carried out at identical volumes. On a glass slide, stained cell suspension was dropped freshly and was screened by a coverslip and observed under the fluorescent microscope 30 minutes prior before fading.[18]

Cell cycle analysis

Prostate cancer cells (PC3) were cultured at the concentration of 2×10^5 cells/mL in RPMI-1640 medium, which was complemented with 1% penicillin/streptomycin and 10% FBS in a 25-mL culture flask (TPP brand). Later, it was treated with various concentrations of biseugenol B for 1 day. The cells were harvested and stained with a BD Cycletest Plus DNA Reagent Kit (BD Biosciences, San Jose, CA, USA) according to the manufacturer's protocol and subjected to cell cycle analysis using a Guava easyCyte 8HT Benchtop Flow Cytometer (Merck & Co., Inc., Whitehouse Station, NJ, USA).[22,25]

Assay of the apoptotic rate by annexin V (AV)-fluorescein isothiocyanate (FITC) staining

A number of prostate cancer cells were cultured (1×10^5) and exposed to different concentrations of biseugenol B. By using the BD Pharmingen™ Annexin V-FITC Apoptosis Detection Kit (APO Alert Annexin V; Clontech, Mountain View, CA, USA),[26] the AV assay was executed. To eliminate the media, treated cells were centrifuged for 5 minutes at 1,800 rpm. In all, 1× binding buffer (provided by the manufacturer) was used to wash the cells. Subsequently, the cells were suspended for the second time in 200 µL of binding buffer, and prior to the incubation at 37°C, which was carried out for 15 min in the dark, 5 µL of AV and 10 µL of PI (Sigma-Aldrich Co, St Louis, MO, USA) was added. The former caused the jump in the volume of the reaction to 500 µL for the analysis of flow cytometric, which was carried out employing FACSCanto II (BD Biosciences) cytometry b. The control applied was the dimethyl sulfoxide-treated (0.1%, v/v) cells.[26]

Multiple cytotoxicity assay

Six independent factors such as changes in cell membrane permeability, nuclear size, cytochrome c release, morphological changes, cell loss and mitochondrial membrane potential (MMP) were quantified in the same time through applying a Multiparameter Cytotoxicity 3 Kit (Cellomics Technology, Halethorpe, MD, USA).[19,27] In brief, prior to treatment with biseugenol B for 1 day, the PC3 cells were seeded and incubated at 37°C during the night with 5% CO_2. Cell permeability dye and also the MMP dye were later added to the mentioned cells, and incubation was carried out for half an hour at the same temperature. Then, fixing, permeabilizing and blocking of the cells were conducted with 1× blocking buffer and subsequently analyzed with initial antibody of cytochrome c and secondary DyLight 649-conjugated goat anti-mouse immunoglobulin G, which took 55 minutes each. In order to stain the nucleus, Hoechst 33342 staining solution was employed and 1,000 stained cells were studied through employing the ArrayScan™ High-Content Screen System (Cellomics Technology; Halethorpe, MD, USA). Stained cells were identified by this system, and the intensity and distribution of fluorescence were reported in individual cells. For each fluorescence channel, special filters were applied for obtained images. Images and data pertaining to the intensity and texture of fluorescence within individual cells, as well as the average fluorescence of the cell population within the well, were stored in the Microsoft SQL database. Later, the factors were all examined by Data Viewer version 3.0 software (Cellomics Technology) and ArrayScan II Data Acquisition.[27]

Bioluminescent assays for caspase activity

Caspase-Glo® assay kits (Promega Corporation, Fitchburg, WI, USA)[28] were used for a dose-dependent study of caspases 3/7, caspase-8 and caspase-9 in triplicate in a 96-well microplate. RWPE-1 in the concentration of 1×10^5 cells/well and PC3 in the concentration of 1×10^4 cells/well were seeded and incubated with various concentrations of biseugenol B for 24 hours. The activity of the caspases was studied and analyzed according to previous studies.[19,29] In brief, the reagent of 100 µL of Caspase-Glo was added and later incubated for half an hour at room temperature. Aminoluciferin-labeled synthetic tetrapeptide was cleaved due to the existence of active caspases from apoptotic cells, followed by discharging the substrate for luciferase enzyme. By using an Infinite M 200 PRO microplate reader (Tecan, Männedorf, Switzerland), the activity of caspases was measured.[30]

Measurement of reactive oxygen species (ROS) generation

By using 2′,7′-dichlorofluorescin diacetate (DCFH-DA), the production of intracellular ROS was measured.[29,31,32] In all, 10 mM of DCFH-DA stock solution in methanol was diluted 500-fold in Hank's balanced salt solution (HBSS; diluted with no additives to yield a 20-μM working solution).

PC3 and RWPE-1 cells were exposed to different concentrations of biseugenol B in a 96-well black plate and then washed with HBSS twice, followed by incubating at 100 μL working solution of DCFH-DA for 30 minutes at 37°C. The results were obtained using a fluorescence microplate reader at 485-nm excitation and 520-nm emission (Infinite M 200 PRO).[33,34]

Analysis of mRNA expression by reverse transcription polymerase chain reaction (RT-PCR)

Prostate cancer cells PC3 were cultured in 12-well plates and treated with different concentrations of biseugenol B. By using RNeasy Mini Kit (Qiagen NV, Venlo, the Netherlands),[19,35] the cells' total RNA was extracted. PCR amplification was performed on 1 μL of transcribed cDNA using specific primers such as Bcl-cell lymphoma (Bcl)-2, heat-shock protein 70 (Hsp70) and Bcl-2-associated X (Bax) genes. β-Actin mRNA was applied as the loading control. The primers for Bcl-2 were sense, 5′-ATG AAC TCT TCC GGG ATG G-3′, and antisense, 5′-TGG ATC CAA GGC TCT AGG TG-3′; Hsp70 were sense, 5′-CGC AGC TGA ACA AGC TAA ACA ATC-3′, and antisense, 5′-GAT TGT TTA GCT TGT TCA GCT GCG-3′; Bax were sense, 5′-TTT GCT TCA GGG TTT CAT CC-3′, and antisense, 5′-GCC ACT CGG AAA AAG ACC TC-3′ and β-actin were sense, 5′-CGG GAA ATC GTG CGT GAC-3′, and antisense, 5′-GCC TAG AAG CAT TTG CGG TG-3′. The amplification of PCR was carried out through a thermal cycle in which the reaction initiated in primary denaturation for 5 minutes at 95°C, which was succeeded by 30 denaturation cycles, which were annealed and extended at 95°C, 60°C and 72°C for 30 seconds, 40 seconds and 1 minute, respectively. Following the last extension, which was carried out at 72°C and lasted for 10 minutes, the reaction came to an end. The amplification product size was 515 bp for β-actin, 213 bp for Bax and 166 bp for Bcl-2. The products of PCR were loaded into 1.5% agarose gel electrophoresis. The staining process was later carried out with ethidium bromide. By the help of UV light employing Gel Doc XR System (Bio-Rad Laboratories Inc., Hercules, CA, USA), the products were visualized.[19]

Western blot analysis

Prostate cancer cells PC3 were cultured in a 25-mL flask (TPP Techno Plastic Products AG, Trasadingen, Switzerland), followed by treating the cells with different concentrations of biseugenol B for 24 hours.[26] Lysis buffer (50 mM Tris-HCL, pH 8.0; 120 mM NaCl; 0.5% NP40; 1 mM phenylmethylsulfonyl fluoride) was used to extract the total protein cell. In all, 10% sodium dodecyl sulfate polyacrylamide gel electrophoresis was used to separate the 40 μg of extracted protein. The separated proteins were transferred to polyvinylidene difluoride membrane (Bio-Rad Laboratories Inc.). Then, proteins were blocked with 5% nonfat milk in tris-buffered saline (TBS) with Tween 20 (TBST) buffer 7 (0.12 M Tris Base, 1.5 M NaCl, 0.1% Tween 20). This stage took 30 minutes and was performed at room temperature followed by incubation by proper primary antibody at 4°C overnight. Subsequently, proteins incubated in alkaline phosphatase conjugated secondary antibody for half an hour at room temperature. The mixture of Tween 20 buffer and TBS was used for washing. Hsp70 (heat shock protein), nuclear factor kappa-B (NF-κB)/P65 (sc-398442), Bax (sc-20067) and β-actin (sc-130300) were purchased from Santa Cruz Biotechnology Inc. (Dallas, TX, USA), while Bcl-2 (ab38629) was purchased from Abcam plc (Cambridge, UK) and served as primary antibodies. For secondary antibodies, we applied alkaline phosphatase-conjugated goat anti-rabbit or goat anti-mouse. Proteins were incubated in a ratio of 1:5,000 of secondary antibody at room temperature for 1 hour. Then, they were washed three times with TBST in an orbital shaker for 10 minutes. By using BCIP®/NBT (Santa Cruz Biotechnology Inc.), the blots were developed for sensitive colorimetric detection to quantify the target protein band.[19,36]

NF-κB translocation

Briefly, 1×10^4 PC3 cells were seeded in a 96-well plate and incubated overnight at 37°C with 5% CO$_2$. The cells were treated with different concentrations of the compound biseugenol B for 3 hours and then stimulated with 10 ng/mL of tumor necrosis factor-alpha (TNF-α) for 30 minutes. Briefly, a number of PC cells (1×10^4) were seeded and incubated in a 96-well plate with 5% CO$_2$ at 37°C. The treatment of the cells with various concentrations of biseugenol B compound was carried out for 180 minutes, followed by stimulation with 10 ng/mL of TNF-α for half an hour. Later, eliminating the medium and fixing the cells, which was followed by staining them with NF-κB activation kit (Thermo Fisher Scientific, Waltham, MA, USA), were carried out based on

the manufacturer's protocol. On an ArrayScan High-Content Screening Reader, the plate was analyzed. Measuring the intensity ratio of nuclear NF-κB as well as the cytoplasm NF-κB was performed by Cytoplasm to Nucleus Translocation BioApplication software (Thermo Fisher Scientific). For 200 cells/well, the quantification of the average intensity was done by comparing different ratios of TNF-α stimulated in untreated and treated cells.[27,37]

Statistical analysis

Regarding the experimental data, the statistical investigation was shown as the mean ± standard deviation for three independent tests. The factors of homogeneity and normality of variance were audited. Statistical Package for the Social Sciences version 19.0 (IBM Corporation, Armonk, NY, USA) and GraphPad Prism version 3.0 (GraphPad Software Inc., La Jolla, CA, USA) software were used. Statistical significance was defined at $P<0.05$.[27]

Results

Biseugenol B inhibits the growth of PC3 cells

The valuation of the effect of biseugenol B on PC3 (prostate cancer cell line) and RWPE-1 (normal prostate cell line) was performed by using MTT assays in a dose-dependent manner (Table 1). The obtained results represent the IC_{50} values after 24, 48, and 72 hours of treatment of PC3 with biseugenol B (Figure 2).

AO–PI double-staining cell morphological analysis

The cells were counted using a fluorescence microscope to investigate the population of viable cells (VI), early apoptosis (EA), late apoptosis (LA), and secondary necrosis. A total of 200 cells were counted arbitrarily and differentially, along with untreated cells, which were considered as negative control. Early apoptosis cells were distinguished with a bright green fluorescence using AO within the fragmented DNA. The control cells were illustrated by the green nuclear structure, which was shown to be intact (Figure 1). Subsequent treatment with 2 µg/mL biseugenol B, nuclear

Table 1 IC_{50} concentration of biseugenol B

Cell line	IC_{50} (µg/mL)		
	24 hours	48 hours	72 hours
PC3	2.42±1.05	2.1±0.38	1.33±0.47
RWPE-1	57.43±1.15	45.65±2.94	34.92±1.6

Note: Data presented as mean ± standard deviation.
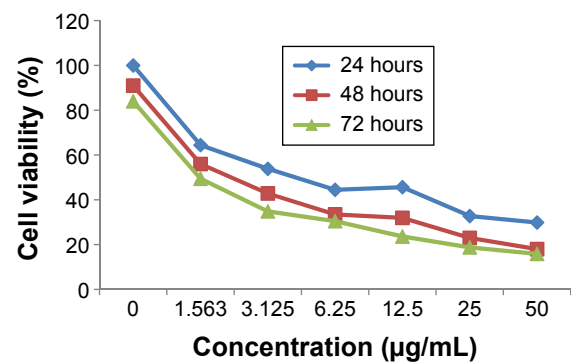**Abbreviation:** IC_{50}, half maximal inhibitory concentration.

Figure 2 MTT assay growth curve of PC3 cells treated with biseugenol B at 24, 48, and 72 hours.
Abbreviation: MTT: 3-(4,5-dimethylthiazol-2-yl)-2,5-diphenyltetrazolium bromide.

chromatin condensation and blebbing detected represent moderate apoptosis (Figure 3A and B). Furthermore, after treatment with 4 and 8 µg/mL of biseugenol B, in the later phases of apoptosis, modifications, including a reddish-orange color due to the binding of AO to the denatured DNA, were observed (Figure 3C and D). The results showed that the biseugenol B shaped morphological features that are associated with apoptosis in a dose-dependent manner.[38] In the cell population, through the differential recording of treated cells (200 cell population), a statistically significant ($P<0.005$) difference was noted (Figure 4).

Effects of biseugenol B on the ratio of apoptotic cells by AV-FITC staining

For confirmation of the apoptotic effects of biseugenol B on PC3 cells, flow cytometric analysis with AV/PI double staining was used. The AV+/PI− staining represents the EA cells due to the affinity strength between AV-FITC and phosphatidylserine, which leads to transportation from inner leaflet to the outer surface of the plasma membrane in EA.[39] In contrast, AV−/PI+ staining represents the necrotic cells, since PI can only pass through the damaged membrane of the dead cells or late apoptotic cells and binds to the nucleic acid. In addition, AV−/PI− staining represents VI, and AV+/PI+ staining is marked as late apoptotic cells (Figure 5A–D) The characteristic dot plots of the flow cytometric assessment of apoptosis indicated that comparing to control (untreated cells), the percentage of EA increases significantly ($P<0.005$) in the treated cells, especially at 4 µg/mL (~20-fold). Also, LA cells upsurge meaningfully ($P<0.005$) at 8 µg/mL (~10-fold) compared to untreated cells (Figure 5E). Moreover, the biseugenol B treatment clearly results in a noteworthy decrease in VI at 4 and 8 µg/mL. Overall, the results demonstrate the anti-proliferative effect of biseugenol B on PC3 cells by triggering the induction of apoptosis cells.
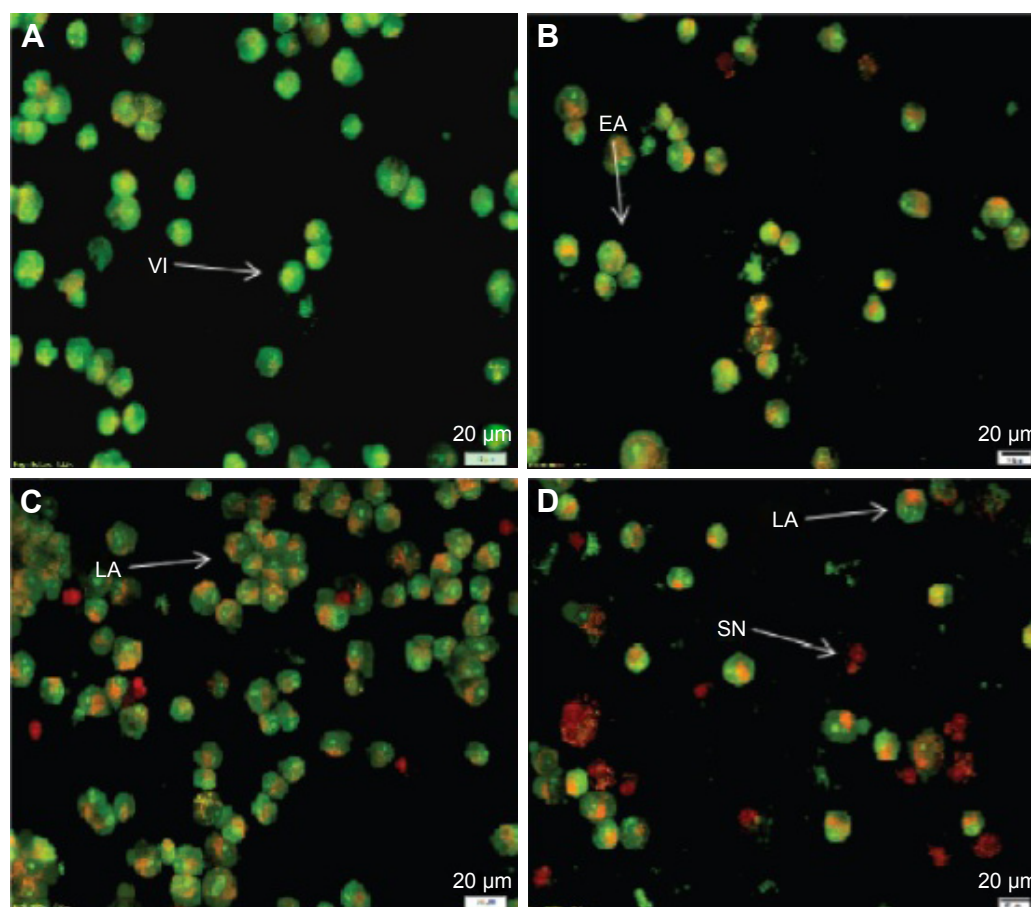
Figure 3 AO-PI double-staining cell morphological analysis in untreated and treated PC3 cells with biseugenol B.

Notes: Normal structure without noticeable apoptosis or necrosis is shown in untreated cells (**A**). After treatment with 2 µg/mL, EA features were observed with intercalated AO (bright green) among the fragmented DNA (**B**). In 4 µg/mL treatment, the hallmark of LA was detected, which is represented by blebbing and orange color (**C**). After treatment with 8 µg/mL, SN was visible by bright red color (**D**).

Abbreviations: AO, acridine orange; VI, viable cells; EA, early apoptosis; LA, late apoptosis; SN, secondary necrosis; PI, propidium iodide.
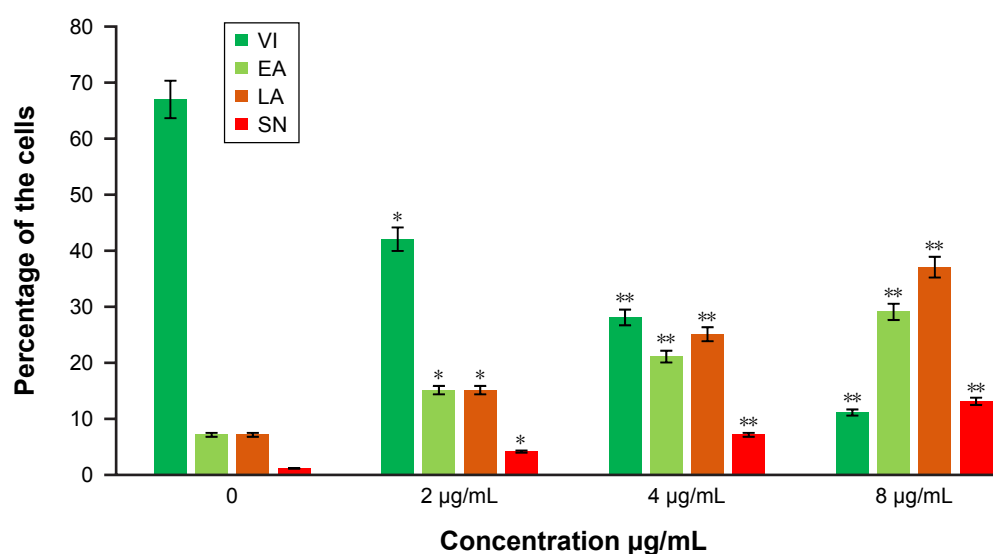
Figure 4 The percentages of VI, EA, LA and SN cells after biseugenol B treatment.

Notes: A significant increase was observed in PC3 cell death via apoptosis in a dose-dependent manner. The results are shown as mean ± SD of three independent experiments. $*P<0.05$. $**P<0.005$.

Abbreviations: VI, viable cells; EA, early apoptosis; LA, late apoptosis; SN, secondary necrosis; SD, standard deviation.
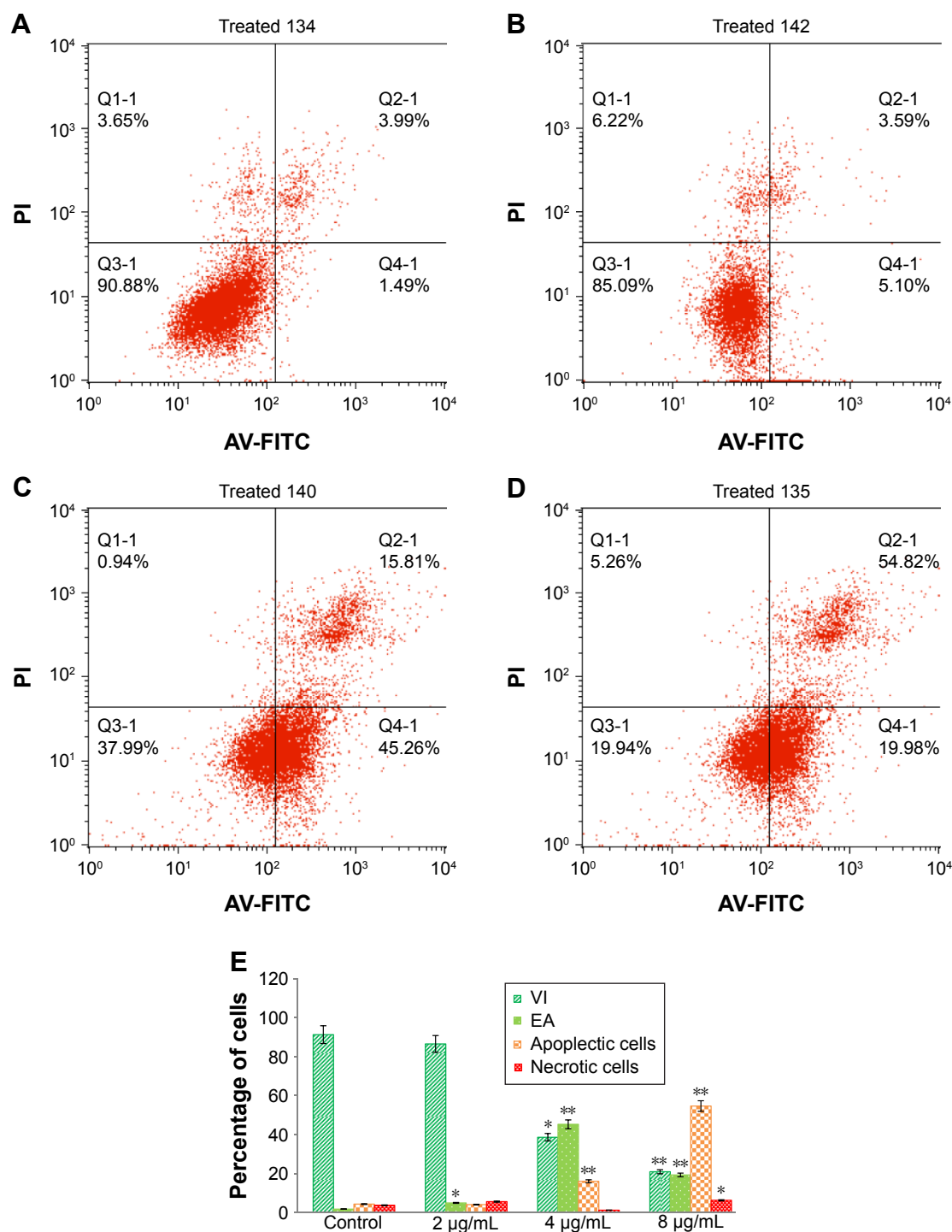
Figure 5 The effect of biseugenol B on EA and LA of PC3 cells.

Notes: PC3 cells were treated with different concentrations of biseugenol B and maintained for 24 hours at 37°C in a CO_2 incubator. The cells were analyzed after staining with FITC-conjugated AV and PI by flow cytometer. Untreated cells served as control (**A**). AV^+/PI^- represents the EA events shown in lower right quadrant (Q4-1). The late stage of apoptosis/dead cells (AV^+/PI^+) is shown in quadrant Q2-1. The effects of 2, 4 and 8 µg/mL exposures of PC3 cells to biseugenol B (**B–D**). Bar chart representing the percentage of VI, EA, LA and necrotic cells in different concentrations of treatment with biseugenol B on PC3 cells (**E**). The results are shown as mean ± SD of three independent experiments. *$P<0.05$. **$P<0.005$.

Abbreviations: EA, early apoptosis; LA, late apoptosis; FITC, fluorescein isothiocyanate; AV, annexin V; PI, propidium iodide; VI, viable cells; SD, standard deviation.

Cell cycle analysis

This experiment was conducted to determine the influence of biseugenol B on the DNA content of PC3 cells by the cell cycle phase distribution (G0, G1, S, G2 and M) after treatment (Figure 6 and Table 2). The results indicated that biseugenol B arrested the cell cycle progression in the G0/G1 phase ($P<0.05$). The results demonstrate a significant G0/G1 phase arrest in a dose-dependent manner in the PC3 cells
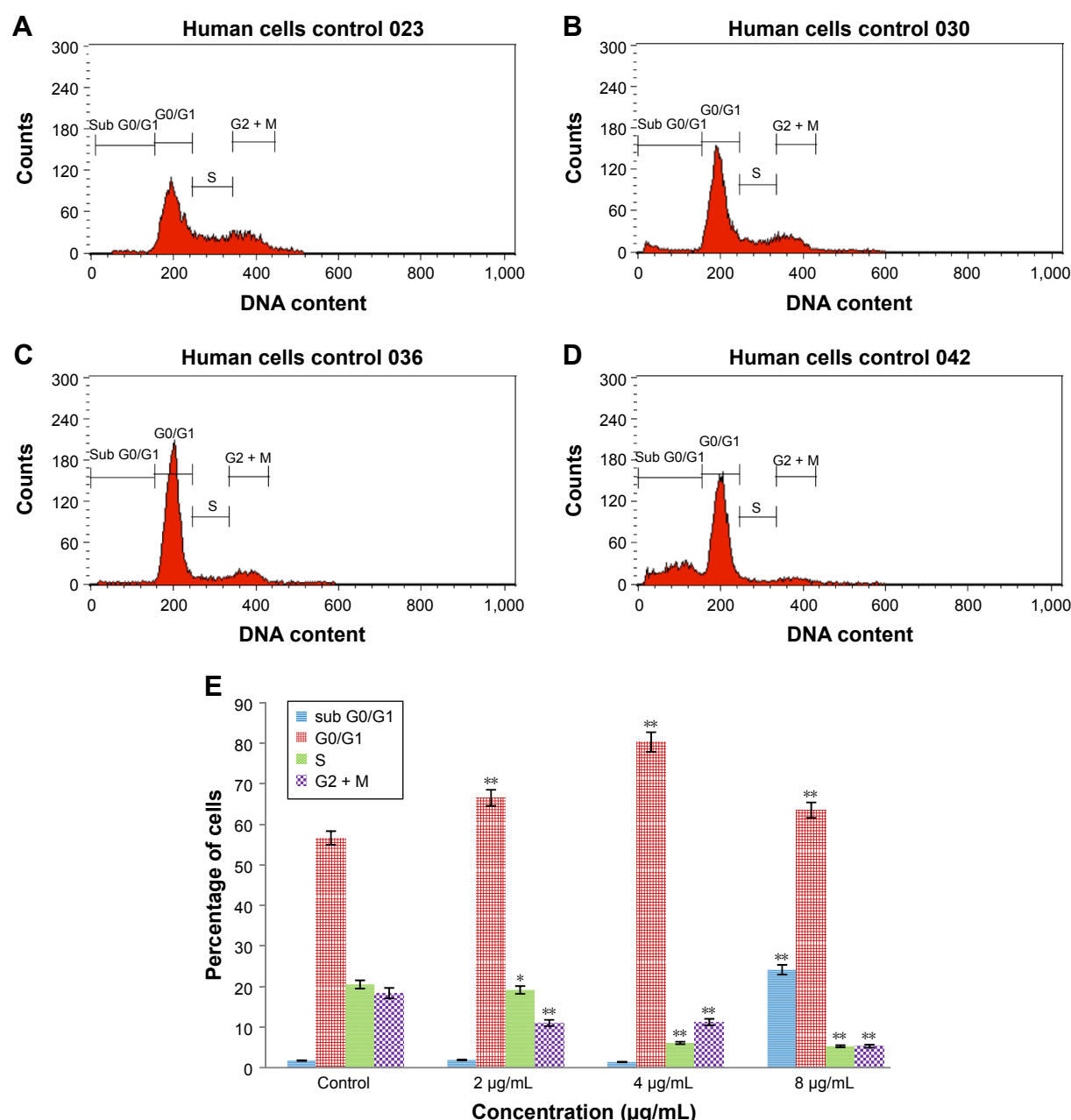
Figure 6 Cell cycle histogram from analyses of PC3 cells treated with 0 μg/mL (**A**), 2 μg/mL (**B**), 4 μg/mL (**C**) and 8 μg/mL (**D**) of biseugenol B for 24 hours. (**E**) Summary of cell cycle progression for control and biseugenol B-treated PC3 cells.
Notes: The results are shown as mean ± SD of three independent experiments. *$P<0.05$. **$P<0.005$.
Abbreviation: SD, standard deviation.

Table 2 Effect of biseugenol B on cell cycle phases

Concentration	Sub G0–G1	G0–G1	S	G2/M
0 μg/mL	1.94±0.32	58.84±1.15	16.45±2.02	8.81±1.65
2 μg/mL	2.47±0.46	66.88±1.58**	18.73±1.38*	10.22±1.06**
4 μg/mL	1.75±0.42	78.06±1.37**	7.77±0.94**	11.22±1.67**
8 μg/mL	24.73±0.24**	64.93±1.04**	3.59±0.55**	5.94±1.48**

Notes: Human prostate cancer cells were exposed to biseugenol B at various concentrations (0, 2, 4, and 8 μg/mL) for 24 hours. The table summarizes the percentages of cells in each phase of the cell cycle after treatment with biseugenol B. Data in the same vertical column but different rows refer to the same phase of the cell cycle and different biseugenol B concentrations. The results are shown as mean ± SD of three independent experiments. *$P<0.05$. **$P<0.005$.
Abbreviation: SD, standard deviation.

(Figure 6E), which accounts for 66.88%, 78.06% and 64.93% of cells, following treatment with 2, 4, and 8 μg/mL, respectively, for 24 hours ($P<0.05$; Table 2). Meanwhile, the cells in both the S and G2/M phases reduced with an increase in the treatment dosage.

Biseugenol B-induced MMP disruption and release of cytochrome c

In the apoptosis, MMP disturbs by insertion of pro-apoptotic proteins such as Bax and BH3 or by making of permeability

transition pores. By using a mitochondria-specific voltage-dependent dye, we detected the effect of biseugenol B on the MMP of PC3 cells. As displayed in Figure 7A and B, a significant reduction ($P<0.005$) was noted in MMP of PC3 cells after treatment with biseugenol B. Also, a noteworthy decline was observed in fluorescence intensity ($P<0.05$), which reflected the break down of MMP. In addition, biseugenol B significantly increased the translocation of cytochrome c from mitochondria into the cytosol ($P<0.005$).

Effect of biseugenol B treatment on caspase-3/7, -8 and -9

The extreme production of ROS from the mitochondria and MMP collapse can activate downstream caspase molecules, leading to apoptotic cell death. For examining the caspase enzyme alteration by biseugenol B, we measured the bioluminescent intensities related to caspase activity in the PC3 and RWPE-1 cells treated with different concentrations of biseugenol B for 24 hours. As shown in Figure 8A, all the caspase enzymes showed significant dose-dependent increase by the biseugenol B treatment in PC3 cells ($P<0.005$). Therefore, apoptosis induced by biseugenol B in PC3 cells is mediated via both intrinsic (mitochondrial caspase-9 pathway) and the extrinsic death receptor-linked caspase-8 pathway. In contrast, the normal prostate cells (RWPE-1) were less sensitive to biseugenol B, showing a mild increase in caspase-3/7, caspase-8 and caspase-9 ($P>0.05$) (Figure 8B). Quantitative analysis confirmed the significant difference between PC3 and RWPE-1 cells in the induction of caspases by biseugenol B. (Figure 8C).
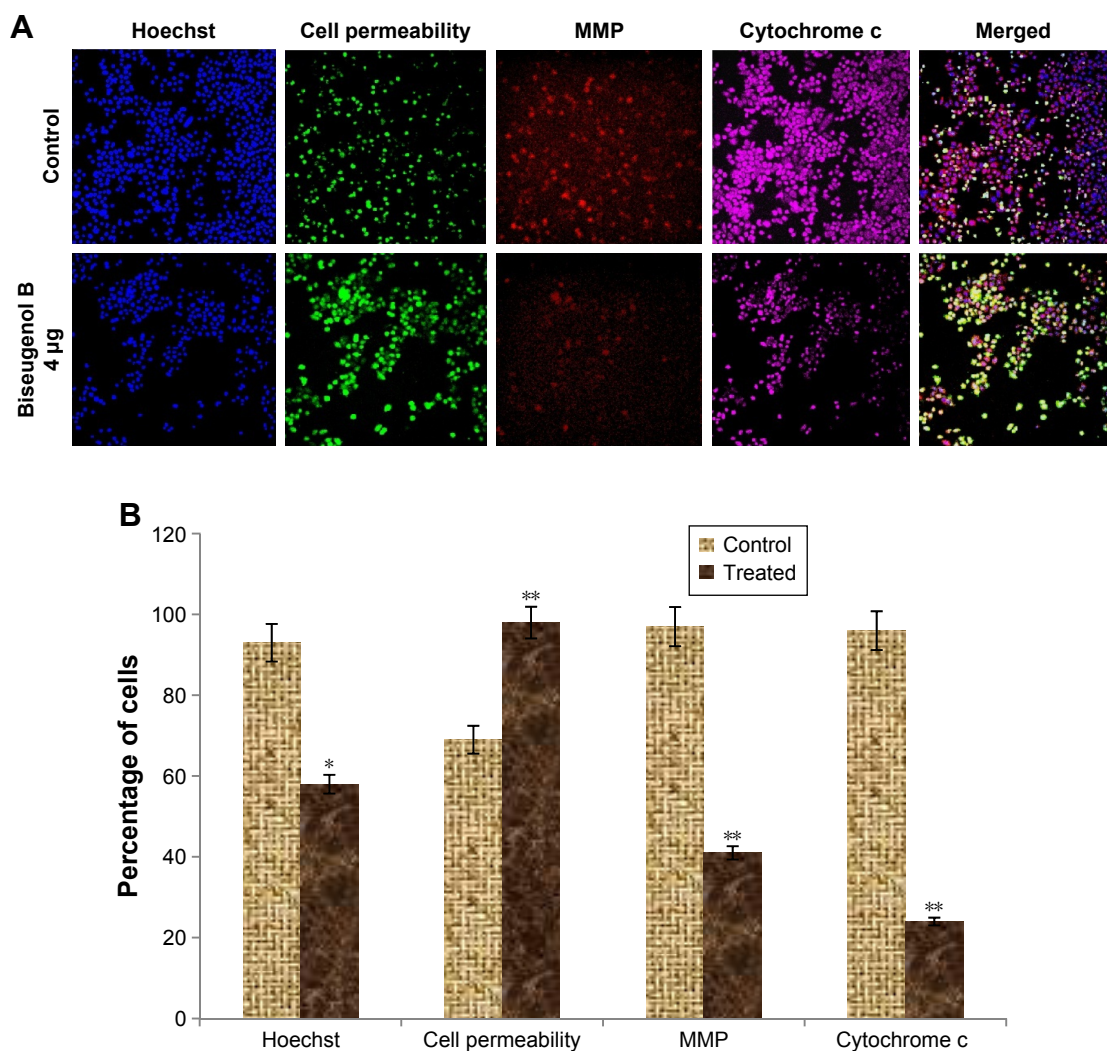

Figure 7 The effect of biseugenol B on nuclear size, MMP, cell membrane permeability, and cytochrome c release in PC3.
Notes: (**A**) Representative images of the untreated PC3 cells and PC3 cells treated with 4 µg/mL biseugenol and stained with Hoechst for nucleus, cytochrome c, membrane permeability and MMP dyes and cytochrome c dye. The images from each row are obtained from the same field of the same treatment sample (magnification ×20). (**B**) The bar chart represents the average fluorescence intensities of Hoechst, cell permeability dye, MMP, and cytochrome c in untreated and treated PC3 cells with biseugenol B. Data are mean ± SD of fluorescence intensity readings measured from different photos taken. *$P<0.05$. **$P<0.005$.
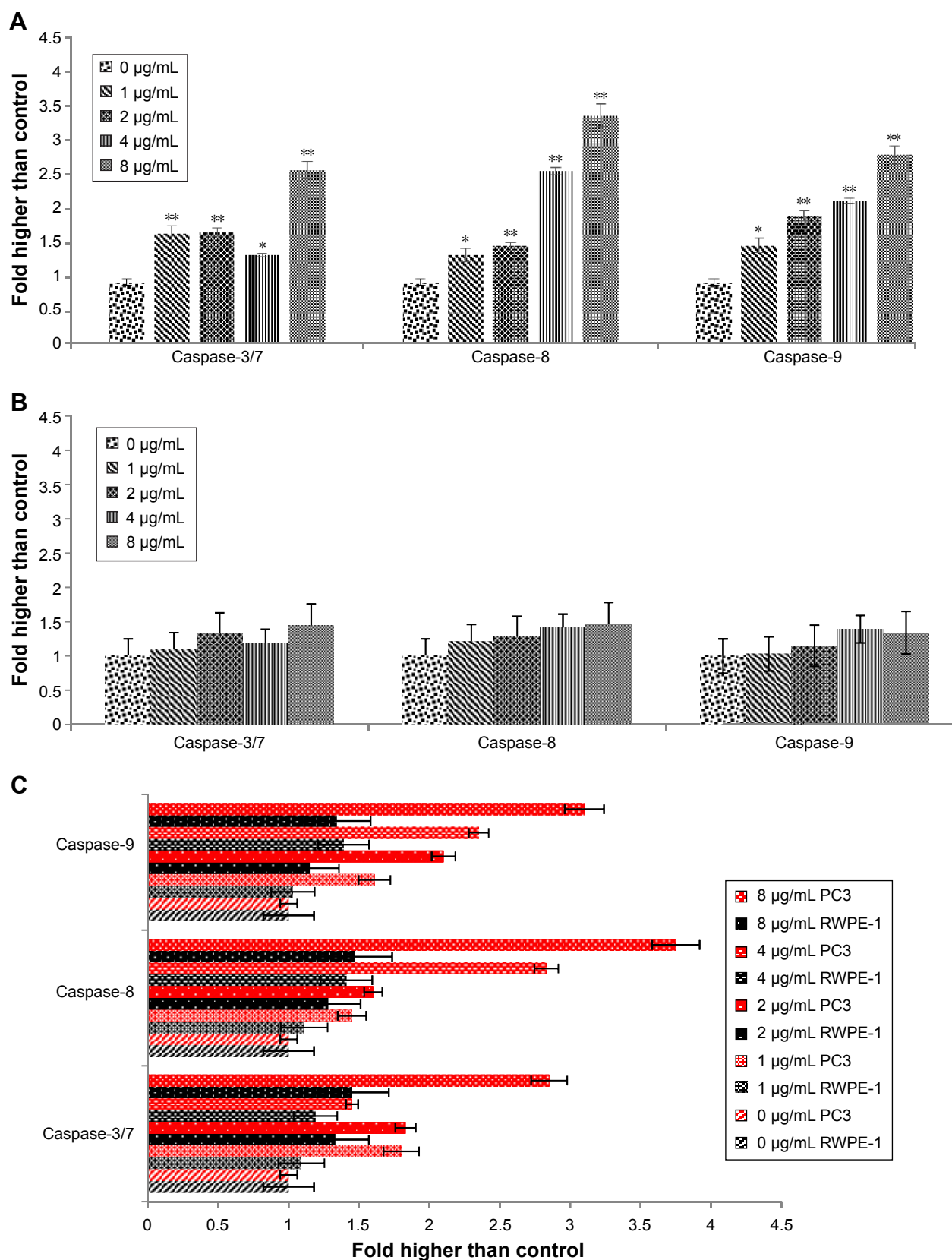**Abbreviations:** MMP, mitochondrial membrane potential; SD, standard deviation.

A

B

C

Figure 8 Relative bioluminescence expression of caspase-3/7, caspase-8, and caspase-9 in PC3 and RWPE-1 cells treated with biseugenol B.
Notes: (**A**) Relative bioluminescence expression of caspase-3/7, caspase-8 and caspase-9 in PC3 cells treated with biseugenol B in different concentrations. The results are shown as mean ± SD of three independent experiments. *$P<0.05$. **$P<0.005$. (**B**) Relative bioluminescence expression of caspase-3/7, caspase-8 and caspase-9 in RWPE-1 cells treated with biseugenol B in different concentrations. The results are shown as mean ± SD of three independent experiments. (**C**) Comparison of relative bioluminescence expression of caspase-3/7, caspase-8, and caspase-9 between PC3 and RWPE-1 cells treated with biseugenol B in different concentrations.
Abbreviation: SD, standard deviation.

Biseugenol B-induced cell death includes increased ROS formation in PC3 cells

The ROS production is generally associated with the MMP disturbance and cell apoptosis.[40] To determine the relation, we examined the level of ROS in cancer prostate cells (PC3) and normal prostate cells (RWPE-1), treated with biseugenol B. Oxidation-sensitive fluorescent dye DCFH-DA was used to observe ROS. A significant increase was observed in treated PC3 cells, in a dose-dependent manner ($P<0.005$).

An immediate and considerable formation of ROS (more than twofold more than control) was detected with 1 and 2 µg/mL treatment, which increased to approximately threefold more than control with a higher concentration of 4 and 8 µg/mL (Figure 9A). On the contrary, no significant increase was detected in normal prostate cells (RWPE-1) after 24 hours of treatment with biseugenol B ($P>0.05$; Figure 9B). These results indicate that biseugenol B triggered the ROS development of prostate cancer cells (PC3), while it has no
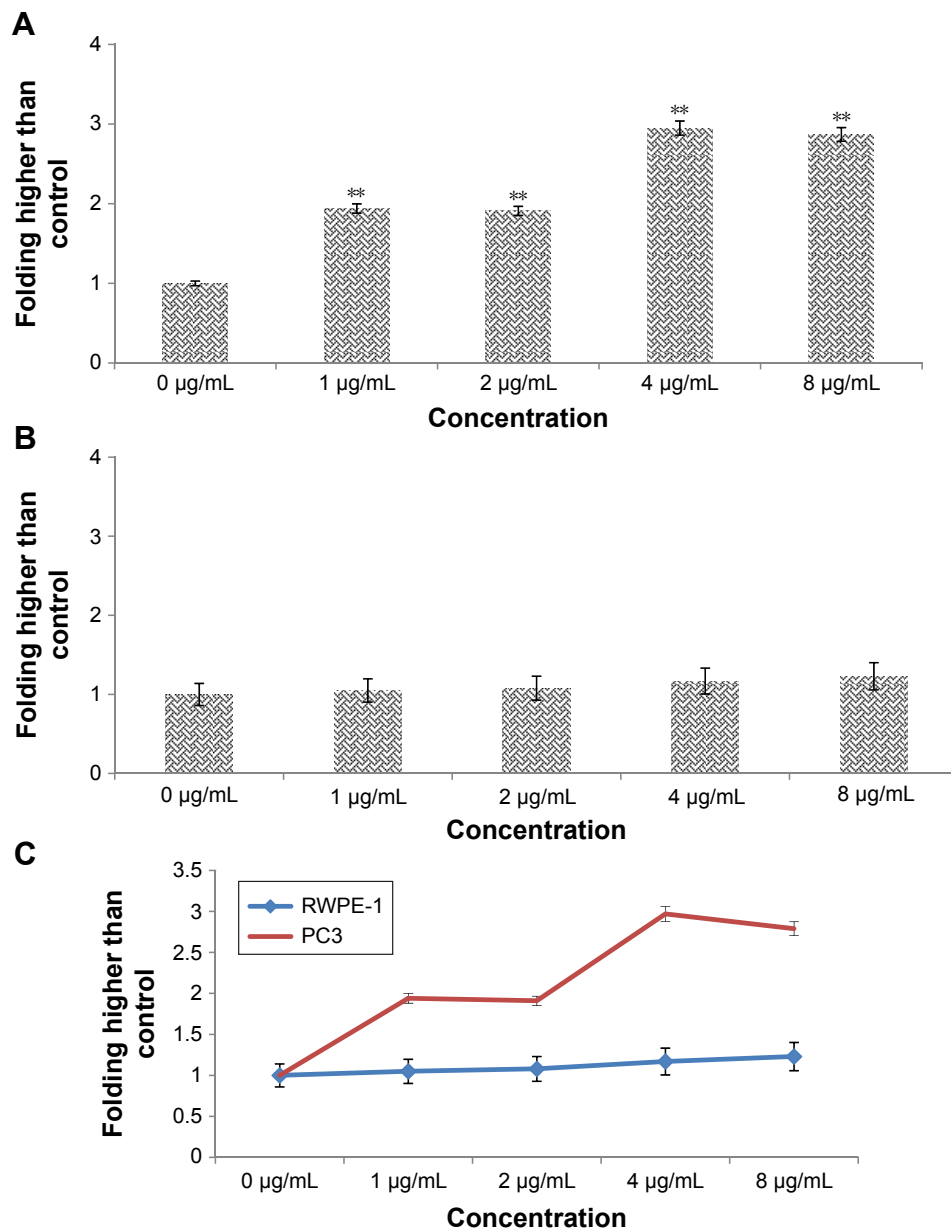

Figure 9 DCF-fluorescence intensity after exposure of biseugenol B for 24 hours in PC3 and RWPE1.
Notes: (**A**) Effects of biseugenol B on PC3 cells in ROS production. DCF-fluorescence intensity after 0, 1, 2, 4 and 8 µg/mL of biseugenol B exposure at 24 hours. The results are shown as mean ± SD of three independent experiments. **$P<0.005$. (**B**) Effects of biseugenol B on RWPE-1 cells in ROS production. DCF-fluorescence intensity after 0, 1, 2, 4 and 8 µg/mL of biseugenol B exposure at 24 hours. The results are shown as mean ± SD of three independent experiments. (**C**) Effects of biseugenol B on PC3 and RWPE-1 cells in ROS production. The results are shown as mean ± SD of three independent experiments.
Abbreviations: ROS, reactive oxygen species; DCF, dichlorodihydrofluorescein; SD, standard deviation.

significant effect on normal prostate cells (RWPE-1). The increase in the ROS production of PC3 and RWPE-1 was seen after 24 hours of treatment with different concentrations of biseugenol B (Figure 9C).

RT-PCR analysis of apoptotic markers

The expression levels of apoptosis markers, Bax (pro-apoptotic), Bcl-2 and Hsp70 (anti-apoptotic), were evaluated by RT-PCR. β-Actin was used as the internal control (Figure 10A). The images represent the changes in apoptotic markers in the treated and untreated cells. The expression of Bax (pro-apoptotic marker) significantly increased by treatment of PC3 cells with biseugenol B ($P<0.05$ for 2 μg/mL of biseugenol B and $P<0.005$ for 4 and 8 μg/mL of biseugenol B; Figure 10B). Furthermore, the expression of Hsp70 and Bcl-2 was significantly downregulated in a dose-dependent manner ($P<0.05$ for 2 μg/mL of biseugenol B and $P<0.005$ for 4 and 8 μg/mL of biseugenol B; Figure 10C and D).

Western blot analysis of apoptotic markers

The results obtained from the Western blot analysis (Figure 11A) confirmed that biseugenol B induced upregulation of Bax significantly ($P<0.05$ for 2 μg/mL of biseugenol B and $P<0.005$ for 4 and 8 μg/mL of biseugenol B; Figure 11B) and downregulation of Bcl-2 and HSP70 proteins in a dose-dependent manner ($P<0.05$ for 2 μg/mL of biseugenol B and $P<0.005$ for 4 and 8 μg/mL of biseugenol B; Figure 11C and D). β-Actin served as the internal control to confirm the equality of sample loading and protein concentration in all samples. The ability of modulation of Bcl-2 and Bax is very crucial for attributing the agent as anticancer, due to their main role in apoptosis regulation; biseugenol B has demonstrated this capability in PC3 cells.

Inhibition of TNF-α-induced NF-κB nuclear translocation by biseugenol B

NF-κB is closely related to the blockage of apoptosis and cell proliferation.[41] Therefore, the role of biseugenol B in
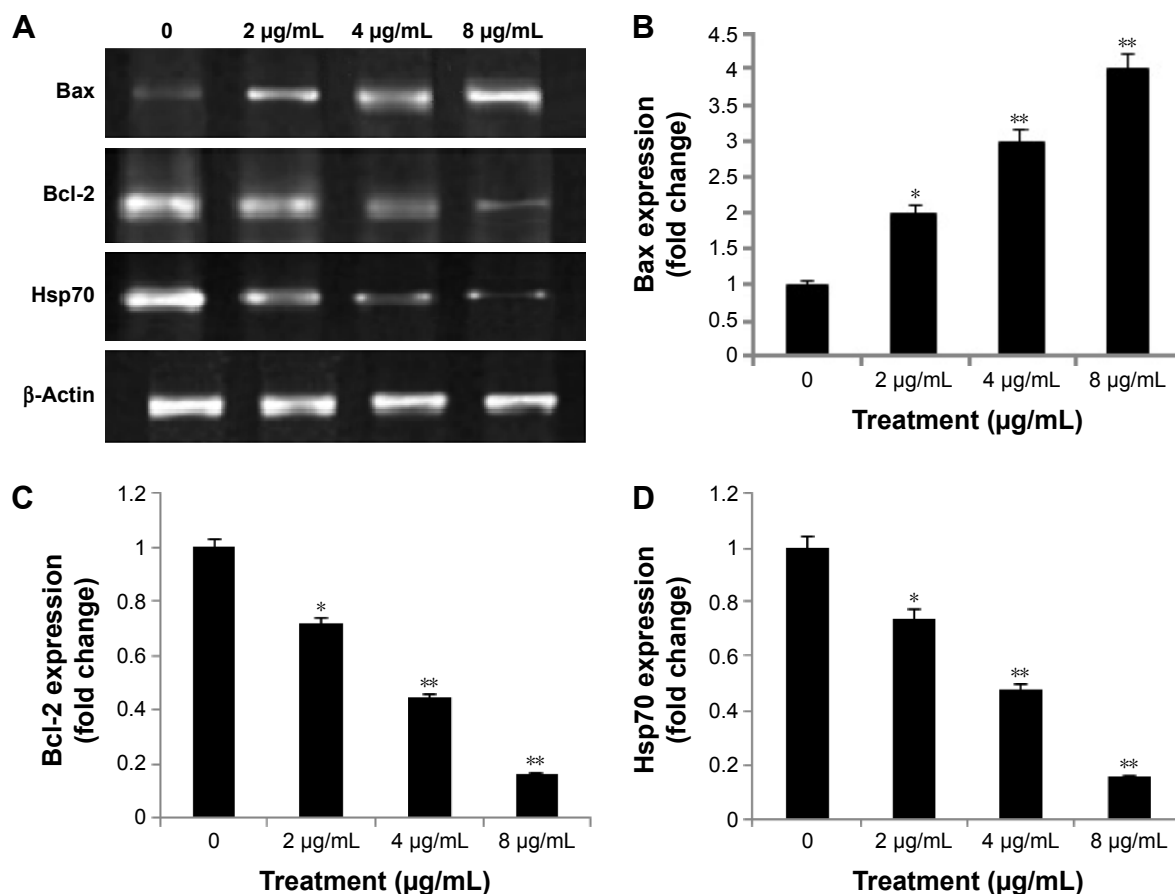

Figure 10 Effects of biseugenol B on the Bax, Bcl-2 and Hsp70 mRNA expression level in PC3 cells.
Notes: PCR analysis of biseugenol B in selected apoptotic signaling markers. The blot densities are expressed as fold of control (**A**). The bar chart represents dose-dependent downregulation of Bax (**B**). The bar charts represent dose-dependent increase of Bcl-2 (**C**) and Hsp70 (**D**). The results are shown as mean ± SD of three independent experiments. *$P<0.05$. **$P<0.005$.
Abbreviations: Bax, Bcl-2-associated X; Bcl-2, Bcl-cell lymphoma-2; Hsp70, heat-shock protein 70; PCR, polymerase chain reaction; SD, standard deviation.
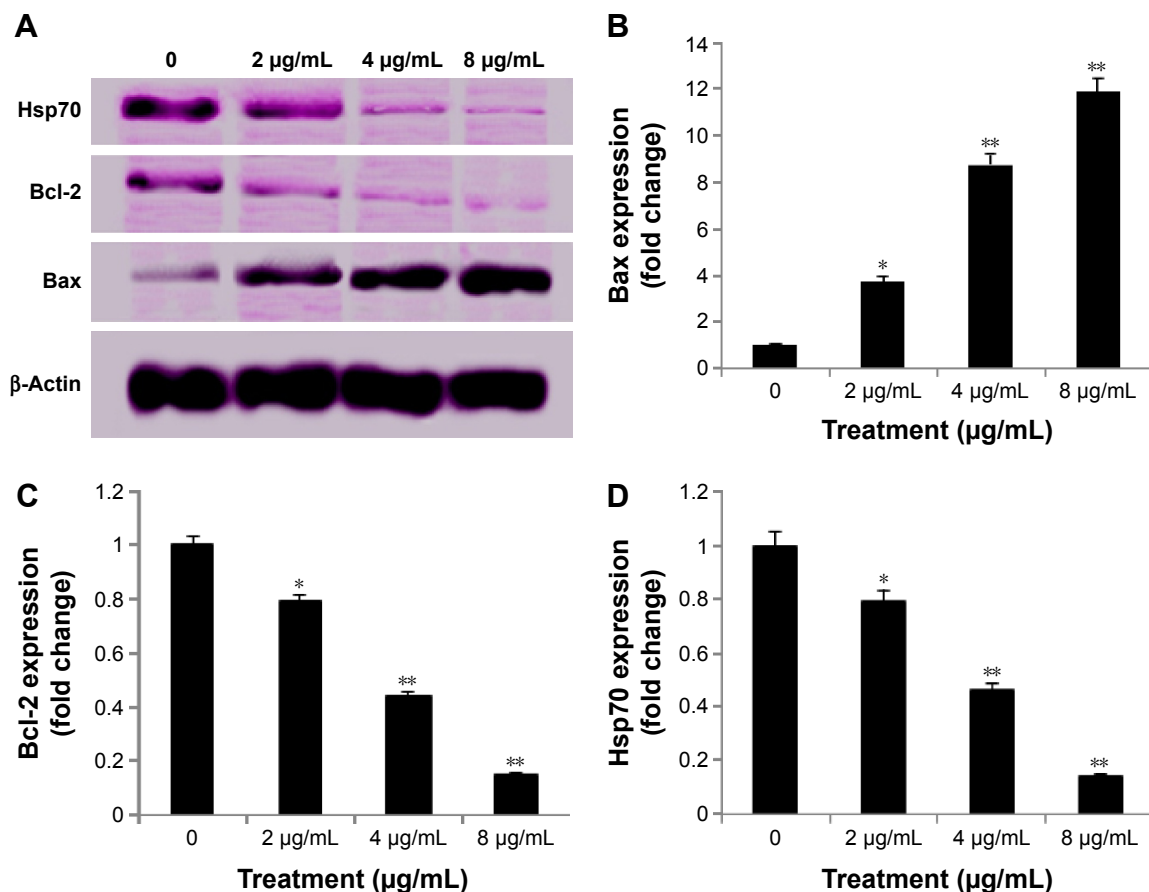
Figure 11 Western blot analysis of biseugenol B in the selected apoptotic signaling markers.
Notes: The blot densities are expressed as fold of control (**A**). Bar chart represents dose-dependent downregulation of Bax (**B**). Bar chart represents dose-dependent increase of Bcl-2 (**C**) and Hsp70 (**D**). The results are shown as mean ± SD of three independent experiments. *$P<0.05$. **$P<0.005$.
Abbreviations: Bax, Bcl-2-associated X; Bcl-2, Bcl-cell lymphoma-2; Hsp70, heat-shock protein 70; SD, standard deviation.

the suppression of activation of NF-κB, induced by TNF-α, was examined. In the control cells, a high NF-κB fluorescent intensity was detected (Figure 12A); the absence of NF-κB activation in the control cells caused the nuclei to have faint color. Followed by adding 10 ng/mL of TNF-α alone to PC3 cells, a considerable NF-κB fluorescent intensity was observed in the nuclei (Figure 12B). Biseugenol B demonstrated a significant inhibition of the triggering of NF-κB (Figure 12C). In the cells treated with well-known NF-κB inhibitors such as curcumin, a considerable suppression of TNF-α-induced NF-κB nuclear translocation has been detected. The NF-κB-related fluorescence intensity was reduced in PC3-TNF-α-stimulated cells (treated with 8 μg/mL of biseugenol B). In addition, immunofluorescence staining demonstrated that the morphological changes of NF-κB translocation indicated the inhibitory effect of biseugenol B on TNF-α-induced NF-κB translocation (Figure 12C). Immunoblotting of the nuclear content of NF-κB p65 was measured to affirm the immunofluorescence result (Figure 13A and B). Treatment with biseugenol B significantly decreased the escalation of

NF-κB p65, induced by positive control (TNF-α) in a dose-dependent manner ($P<0.05$ in PC3 treated with 2 μg/mL of biseugenol B and $P<0.005$ in PC3 treated with 4 and 8 μg/mL of biseugenol B).

Discussion

Apoptosis is an extremely controlled process that plays an essential role in cell destruction and has a crucial role in various cell functions from fetal development to adult tissue homeostasis.[9] Tumors occur through reduction of cell apoptosis and unrestrained cell proliferation. Thus, one of the most logical methods of cancer therapy is using cytotoxic drugs that activate the apoptosis pathway to destroy cancer cells.[42] Herbal medicine is the major source of apoptosis-inducing agents.[43] As stated by several reports,[44–47] many natural compounds may be associated with human cancer therapy, which can induce apoptosis in cancer cells.[48] Apoptosis is related to several biochemical changes in cells, including nuclear fragmentation, change in the MMP, and regulation of caspases.[49] The current study is the first in vitro report of the effect of
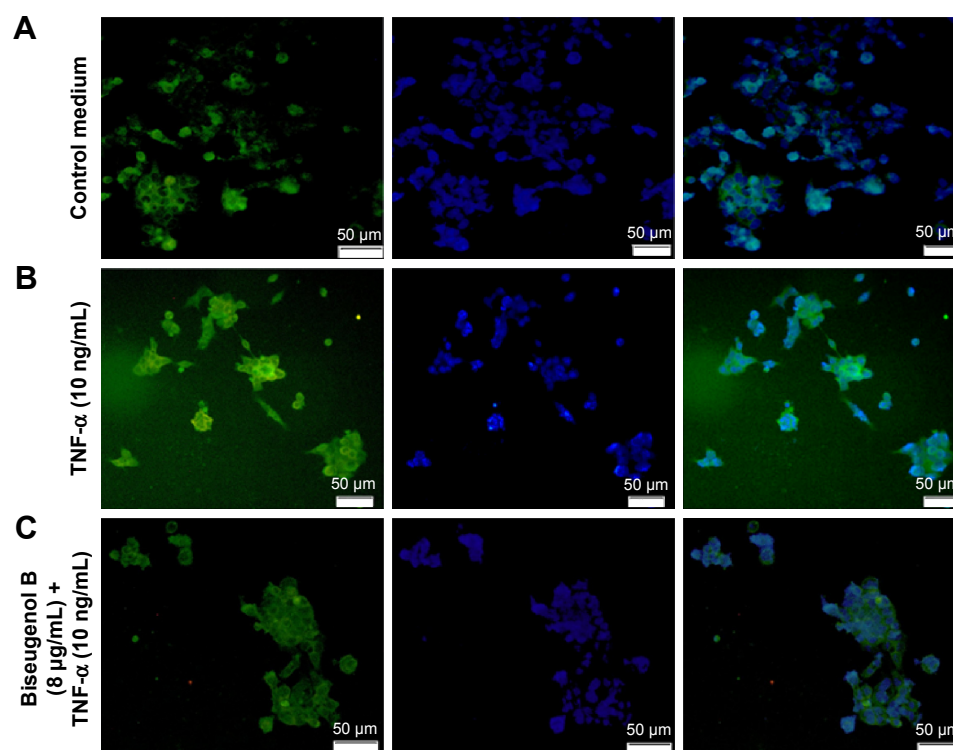
Figure 12 Inhibition of TNF-α-induced NF-κB nuclear translocation by biseugenol B.
Notes: Photographs of intracellular targets in stained PC3 cells treated with biseugenol B for 3 hours (**A**) and then stimulated for 30 minutes with TNF-α 10 ng/mL (NF-κB activation) (**B**). Decline in average fluorescent intensity of nuclei NF-κB, confirming that biseugenol B inhibited TNF-α-induced translocation of NF-κB from the cytoplasm to the nucleus (**C**).
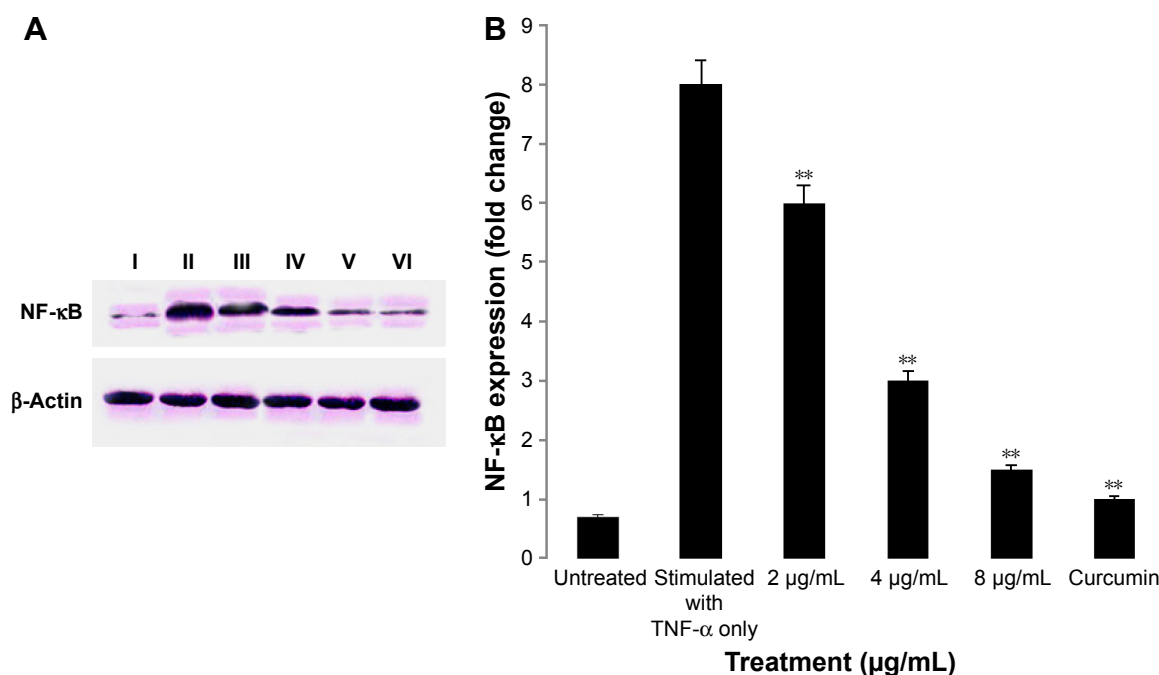**Abbreviations:** TNF-α, tumor necrosis factor-alpha; NF-κB, nuclear factor kappa-B.

Figure 13 Immunoblot analysis of nuclear NF-κB.
Notes: (**A**) Immunoblot analysis of nuclear NF-κB p65. I, untreated PC3; II, stimulated with TNF-α only; III, IV and V, PC3 treated with 2, 4 and 8 µg/mL of biseugenol B, respectively; VI, PC3 treated with curcumin. (**B**) Representative bar chart indicating a significant decline of nuclear NF-κB p65 expressed as folds of control. The results are shown as mean ± SD of three independent experiments. **$P < 0.005$.
Abbreviations: NF-κB, nuclear factor kappa-B; SD, standard deviation.

biseugenol B, a natural compound derived from plant *L. costalis*, against human prostate cancer cells (PC3).

L. costalis, a well-known plant[5] that contains biologically active and structurally diverse aporphinealkaloids,[50–52] has been used to treat various diseases.[53] The natural compound biseugenol B is a major N6-isopentenyladenosine isolated from *L. costalis* (iPA). The present study elucidates the mechanism of apoptosis triggered by biseugenol B on PC3 cells. According to Shier,[54] compounds with IC_{50} value of >30 µg/mL are considered as not potentially cytotoxic, whereas compounds with IC_{50} value of <5.0 µg/mL are considered highly cytotoxic. These findings show that biseugenol B has different effects on normal cells compared with cancer cells; it is more highly cytotoxic on prostate cancer cells (PC3) than on normal prostate cells (RWPE-1).

Since biseugenol B has a strong potential cytotoxic effect on prostate cancer cells, we applied AO and PI fluorescent dyes to observe the various stages of apoptosis, starting with chromatin condensation until apoptotic body formation, with biseugenol B treatment. Although AO/PI clearly featured the apoptosis morphologic changes, we conducted AV assay to quantify the population of apoptotic cells. The current study established that treatment with biseugenol B can induce cell death in PC3 cells through apoptosis. In addition, the results exposed a significant dose-dependent increase in both early and late stages of apoptosis.

Previous studies suggest that oxidative stress has a role in mitochondria change and apoptosis.[55] We measured the ROS level upon biseugenol B treatment on PC3 and RWPE-1 to check the involvement of ROS in the apoptosis process. The results accentuate this significant relation for PC3 ($P<0.05$) but no significant relation for RWPE-1 ($P>0.05$). The results showed a threefold increase in intracellular ROS with 4 and 8 µg/mL of biseugenol B treatment on PC3 cells, which could be due to the generation of free radicals during cytotoxicity.

The apoptosis mode, which can be caused by various natural compounds, is closely associated with the cell cycle arrest.[56,57] Cell cycle control has been proven to be a safeguard for accurate cellular division. Many carcinogenic processes have been proven to cause cell cycle deregulation. Thus, one of the chemotherapy targets in cancer therapy is alteration of cell cycle regulators in cancer cells.[58–60] With various concentrations of biseugenol B, the cell cycle examination of PC3 revealed a significant increase in the number of cells in the sub-G0 phase with the highest concentration of biseugenol B and a larger number of cells in the G0/G1 phase. Alternatively, the number of cells decreased in the S and G2/M phases compared with the untreated cells (Figure 5). The results indicate the inhibitory ability of biseugenol B in cellular proliferation through the G0/G1 phase arrest.

Although both extrinsic and intrinsic pathways are associated with apoptosis, the intrinsic pathway is more frequently involved in tumor occurrence.[25] Mitochondria can directly initiate the apoptosis cellular pathway, so they are considered as the core organelles for the intrinsic apoptosis pathway. Mitochondria can execute multiple cellular functions, but their primary involvement is in cell redox status.[61,62]

Outer membrane permeabilization and mitochondrial transmembrane potential alteration are necessary to initiate the apoptotic cascade and release of pro-apoptotic proteins, including cytochrome c, which eventually results in the activation of caspase-9 and -3.[63] The decrease in mitochondria membrane potential (MMP) is essential for the beginning of the apoptosis process. The fluorescence-based high-content screening analysis revealed the effect of biseugenol B on the mitochondria, which has less MMP in PC3 cells. Simultaneously, the release of cytochrome c also increased.

The key regulatory factor in apoptosis is caspase activation.[64] In the intrinsic pathway, the release of cytochrome c from mitochondria into the cytosol leads to the formation of apoptosome and activates caspase-9, resulting in the activation of effector caspases such as caspase-3, caspase-6 and caspase-7.[65–67] Moreover, previous studies showed that Bcl-2 protein family members mediate the release of cytochrome c in the context of apoptotic stimuli.[68,69] Additionally, movement of Bax into the mitochondria leads to the release of cytochrome c into the cytosol, loss of MMP and induction of mitochondrial permeability transition events.[70] Biseugenol B clearly triggered the release of cytochrome c and increased the activity of caspase-3/7 and caspase-9, which obviously demonstrates that apoptosis was via intrinsic pathway. However, the extrinsic apoptosis pathway of caspase activation involves signal transduction through cell-death receptors such as Fas and TNF-α, resulting in activation of caspase-8, which consequently leads to the activation of downstream effector caspases, such as caspase-3 and caspase-7.[19,71] Activation of caspase-8 is closely involved with extrinsic apoptosis signaling pathway[67] and might interlink with the mitochondrial pathway via cleavage of Bid to tBid.[72] Interestingly, biseugenol B increased the activation of caspase-8 as well, which clearly demonstrates that apoptosis occurs via extrinsic pathway also. On the other hand, no significant increase was observed in RWPE-1 cells by biseugenol B treatment even in the greatest concentration of 8 µg/mL ($P>0.05$).

Concomitantly, certain members of the Bcl-2 family, such as Bcl-2 and Bax, have been identified to control the apoptosis process.[73] The balance between the anti-apoptotic and pro-apoptotic properties of the Bcl-2 family is crucial in actuating the cell toward apoptosis.[74] Previous studies have shown that the upregulation of Bax and downregulation of Bcl-2 cause susceptibility to mitochondria-mediated apoptosis.[75,76] Therefore, we inspected the effect of biseugenol B on the expression of the Bcl-2 family. Bcl-2 is an anti-apoptosis protein located in the cytoplasm, and it plays a significant role in apoptosis inhibition.[77,78] Together with Bcl-2 family members, Hsps are also considered as apoptosis inhibitors, due to their significant role in cell survival.[79] The PCR and Western blot results in this study indicated the Bcl-2 and Hsp70 downregulation in PC3 cells after treatment with biseugenol B in a dose-dependent manner, which can explain the apoptosis-inducing effect of biseugenol B on PC3 cells. In addition, the downregulation effect of biseugenol B on PC3 could be associated with apoptosis factors that are produced in mitochondria and ultimately result in apoptosis.[80]

NF-κB is a protein complex that has a role in regulating DNA transcription and is considered as an apoptosis inhibitor.[81,82] Therefore, repressing the activity of NF-κB can induce apoptosis. In this study, we demonstrated that biseugenol B can repress the apoptosis-inhibitor activity of NF-κB by preventing its translocation from the cytoplasm to the nucleus of the PC3 cells. This finding suggests that biseugenol B can induce apoptosis by suppressing the TNF-α-induced NF-κB anti-apoptosis signaling pathway.

Conclusion

Based on the observations from this study, biseugenol B is capable of inducing apoptosis in PC3 cells through the apoptosis signaling pathway that regulates MMP via downregulation of Bcl-2 and upregulation of Bax, which can cause the release of cytochrome c from mitochondria to cytosol. Upon the release of cytochrome c into the cytosol, caspase-9 is activated, which in turn activates the downstream executioner caspase-3/7. Thereafter, the apoptosis cascade occurs in the cell by slicing specific substrates. Meanwhile, the increase in caspase-8 reveals the involvement of extrinsic pathways. These findings suggest that apoptosis occurs through both intrinsic and extrinsic apoptosis pathways with regulation of NF-κB, Bax, Bcl-2 and Hsp70 protein modulation.

Acknowledgments

The abstract of this paper was presented at the 12th MPS Pharmacy Scientific Conference, 13–15 November 2015, at Taylor's University, Selangor, Malaysia (http://www.cornerstone.com.my/mpspsc2015/), as a poster presentation with interim findings. The poster's abstract was published in "Poster Abstract" of *Malaysian Journal of Pharmacy*.

Disclosure

The authors report no conflicts of interest in this work.

References

1. World Health Organization. *WHO Handbook for Guideline Development*. Geneva: World Health Organization; 2014.
2. Romaguera D, Vergnaud A-C, Peeters PH, et al. Is concordance with World Cancer Research Fund/American Institute for Cancer Research guidelines for cancer prevention related to subsequent risk of cancer? Results from the EPIC study. *Am J Clin Nutr*. 2012;96(1):150–163.
3. Namiki M, Akaza H, Lee SE, et al. Prostate cancer working group report. *Jpn J Clin Oncol*. 2010;40(suppl 1):i70–i75.
4. Benson AB, Schrag D, Somerfield MR, et al. American Society of Clinical Oncology recommendations on adjuvant chemotherapy for stage II colon cancer. *J Clin Oncol*. 2004;22(16):3408–3419.
5. Shukla Y, George J. Combinatorial strategies employing nutraceuticals for cancer development. *Ann N Y Acad Sci*. 2011;1229(1):162–175.
6. Cragg GM, Newman DJ. Natural products: a continuing source of novel drug leads. *Biochim Biophys Acta*. 2013;1830(6):3670–3695.
7. Tang J, Feng Y, Tsao S, Wang N, Curtain R, Wang Y. Berberine and Coptidis rhizoma as novel antineoplastic agents: a review of traditional use and biomedical investigations. *J Ethnopharmacol*. 2009;126(1):5–17.
8. Yan X, Zhang F, Xie H, Wei X. A review of the studies on chemical constituents from Litsea Lam. *J Trop Subtrop Botany*. 1999;8(2):171–176.
9. Jiang Z, Akhtar Y, Bradbury R, Zhang X, Isman MB. Comparative toxicity of essential oils of Litsea pungens and *Litsea cubeba* and blends of their major constituents against the cabbage looper, Trichoplusia ni. *J Agric Food Chem*. 2009;57(11):4833–4837.
10. Yuan YV, Rickard SE, Thompson LU. Short-term feeding of flaxseed or its lignan has minor influence on in vivo hepatic antioxidant status in young rats. *Nutr Res*. 1999;19(8):1233–1243.
11. Beejmohun V, Fliniaux O, Hano C, et al. Coniferin dimerisation in lignan biosynthesis in flax cells. *Phytochemistry*. 2007;68(22):2744–2752.
12. Tavakolinia F, Baghipour T, Hossaini Z, Zareyee D, Khalilzadeh MA, Rajabi M. Antiproliferative activity of novel thiopyran analogs on MCF-7 breast and HCT-15 colon cancer cells: synthesis, cytotoxicity, cell cycle analysis, and DNA-binding. *Nucleic Acid Ther*. 2012;22(4):265–270.
13. Rajabi M, Khalilzadeh MA, Mehrzad J. Antiproliferative activity of novel derivative of thiopyran on breast and colon cancer lines and DNA binding. *DNA Cell Biol*. 2012;31(1):128–134.
14. Hahm J-C, Lee I-K, Kang W-K, Kim S-U, Ahn Y-J. Cytotoxicity of neolignans identified in *Saururus chinensis* towards human cancer cell lines. *Planta Med*. 2005;71(5):464–469.
15. Song S-Y, Lee I, Park C, Lee H, Hahm J-C, Kang WK. Neolignans from *Saururus chinensis* inhibit PC-3 prostate cancer cell growth via apoptosis and senescence-like mechanisms. *Int J Mol Med*. 2005;16(4):517–523.
16. Longato GB, Rizzo LY, Sousa I, et al. In vitro and in vivo anticancer activity of extracts, fractions, and eupomatenoid-5 obtained from *Piper regnellii* leaves. *Planta Med*. 2011;77(13):1482–1488.
17. Hosseinzadeh M, Mohamad J, Khalilzadeh MA, Zardoost MR, Haak J, Rajabi M. Isolation and characterization of bioactive compounds from the bark of *Litsea costalis*. *J Photochem Photobiol B Biol*. 2013;128:85–91.
18. Ali R, Alabsi AM, Ali AM, et al. Cytolytic effects and apoptosis induction of Newcastle disease virus strain AF2240 on anaplastic astrocytoma brain tumor cell line. *Neurochem Res*. 2011;36(11):2051–2062.

19. Mohan S, Abdelwahab SI, Kamalidehghan B, et al. Involvement of NF-κB and Bcl2/Bax signaling pathways in the apoptosis of MCF7 cells induced by a xanthone compound Pyranocycloartobiloxanthone A. *Phytomedicine*. 2012;19(11):1007–1015.

20. Anasamy T, Abdul AB, Sukari MA, et al. A phenylbutenoid dimer, cis-3-(3′,4′-dimethoxyphenyl)-4-[(E)-3‴,4‴-dimethoxystyryl] cyclohex-1-ene, exhibits apoptogenic properties in T-acute lymphoblastic leukemia cells via induction of p53-independent mitochondrial signalling pathway. *Evid Based Complement Alternat Med*. 2013;2013:939810.

21. Nyberg WA, Espinosa A. Imiquimod induces ER stress and Ca 2+ influx independently of TLR7 and TLR8. *Biochem Biophys Res Commun*. 2016;473(4):789–794.

22. Achanzar WE, Diwan BA, Liu J, Quader ST, Webber MM, Waalkes MP. Cadmium-induced malignant transformation of human prostate epithelial cells. *Cancer Res*. 2001;61(2):455–458.

23. Gnanasekar M, Thirugnanam S, Ramaswamy K. Short hairpin RNA (shRNA) constructs targeting high mobility group box-1 (HMGB1) expression leads to inhibition of prostate cancer cell survival and apoptosis. *Int J Oncol*. 2009;34(2):425–431.

24. Gummadi VR, Rajagopalan S, Looi C-Y, et al. Discovery of 7-azaindole based anaplastic lymphoma kinase (ALK) inhibitors: wild type and mutant (L1196M) active compounds with unique binding mode. *Bioorg Med Chem Lett*. 2013;23(17):4911–4918.

25. Chen HW, Huang HC. Effect of curcumin on cell cycle progression and apoptosis in vascular smooth muscle cells. *Br J Pharmacol*. 1998;124(6):1029–1040.

26. Ibrahim MY, Hashim NM, Mohan S, et al. α-Mangostin from *Cratoxylum arborescens* demonstrates apoptogenesis in MCF-7 with regulation of NF-κB and Hsp70 protein modulation in vitro, and tumor reduction in vivo. *Drug Des Devel Ther*. 2014;8:1629.

27. Ahmadipour F, Noordin MI, Mohan S, et al. Koenimbin, a natural dietary compound of *Murraya koenigii* (L) Spreng: inhibition of MCF7 breast cancer cells and targeting of derived MCF7 breast cancer stem cells (CD44+/CD24−/low): an in vitro study. *Drug Des Devel Ther*. 2015;9:1193.

28. Lo Y-L. A potential daidzein derivative enhances cytotoxicity of epirubicin on human colon adenocarcinoma caco-2 cells. *Int J Mol Sci*. 2012;14(1):158–176.

29. Ng K-B, Bustamam A, Sukari MA, et al. Induction of selective cytotoxicity and apoptosis in human T4-lymphoblastoid cell line (CEMss) by boesenbergin a isolated from boesenbergia rotunda rhizomes involves mitochondrial pathway, activation of caspase 3 and G2/M phase cell cycle arrest. *BMC Complement Altern Med*. 2013;13(1):41.

30. Paydar M, Kamalidehghan B, Wong YL, Wong WF, Looi CY, Mustafa MR. Evaluation of cytotoxic and chemotherapeutic properties of boldine in breast cancer using in vitro and in vivo models. *Drug Des Devel Ther*. 2014;8:719–733.

31. Zhang X, Wei H, Liu Z, et al. A novel protoapigenone analog RY10-4 induces breast cancer MCF-7 cell death through autophagy via the Akt/mTOR pathway. *Toxicol Appl Pharmacol*. 2013;270(2):122–128.

32. Kamalidehghan B, Dehghan F, Yahayu M. Involvement of nF-κB and hsP70 signaling pathways in the apoptosis of MDa-MB-231 cells induced by a prenylated xanthone compound, α-mangostin, from *Cratoxylum arborescens*. *Drug Des Devel Ther*. 2014;8:2193–2211.

33. Arbab IA, Abdul AB, Sukari MA, et al. Dentatin isolated from *Clausena excavata* induces apoptosis in MCF-7 cells through the intrinsic pathway with involvement of NF-κB signalling and G0/G1 cell cycle arrest: a bioassay-guided approach. *J Ethnopharmacol*. 2013;145(1):343–354.

34. Zahoor Z, Davies AJ, Kirk RS, Rollinson D, Walker AJ. Nitric oxide production by *Biomphalaria glabrata* haemocytes: effects of *Schistosoma mansoni* ESPs and regulation through the extracellular signal-regulated kinase pathway. *Parasit Vectors*. 2009;2(1):1.

35. Wang W-H, Chiang I, Ding K, et al. Curcumin-induced apoptosis in human hepatocellular carcinoma J5 cells: critical role of Ca(+2)-dependent pathway. *Evid Based Complement Alternat Med*. 2012;2012:512907.

36. Ye M, Liu J-K, Lu Z-X, et al. Grifolin, a potential antitumor natural product from the mushroom *Albatrellus confluens*, inhibits tumor cell growth by inducing apoptosis in vitro. *FEBS Lett*. 2005;579(16):3437–3443.

37. Arbab IA, Looi CY, Abdul AB, et al. Dentatin induces apoptosis in prostate cancer cells via Bcl-2, Bcl-xL, Survivin downregulation, caspase-9, -3/7 activation, and NF-κB inhibition. *Evid Based Complement Alternat Med*. 2012;2012:856029.

38. Moghadamtousi SZ, Kadir HA, Paydar M, Rouhollahi E, Karimian H. Annona muricata leaves induced apoptosis in A549 cells through mitochondrial-mediated pathway and involvement of NF-κB. *BMC Complement Altern Med*. 2014;14(1):1.

39. Salim LZA, Mohan S, Othman R, et al. Thymoquinone induces mitochondria-mediated apoptosis in acute lymphoblastic leukaemia in vitro. *Molecules*. 2013;18(9):11219–11240.

40. Circu ML, Aw TY. Reactive oxygen species, cellular redox systems, and apoptosis. *Free Radic Biol Med*. 2010;48(6):749–762.

41. Prasad S, Ravindran J, Aggarwal BB. NF-κB and cancer: how intimate is this relationship. *Mol Cell Biochem*. 2010;336(1–2):25–37.

42. Shi Y, Zhang L, Liu X, et al. Icotinib versus gefitinib in previously treated advanced non-small-cell lung cancer (ICOGEN): a randomised, double-blind phase 3 non-inferiority trial. *Lancet Oncol*. 2013;14(10):953–961.

43. Di Maro A, Pacifico S, Fiorentino A, et al. Raviscanina wild asparagus (*Asparagus acutifolius* L.): a nutritionally valuable crop with anti-oxidant and antiproliferative properties. *Food Res Intern*. 2013;53(1):180–188.

44. Bhanot A, Sharma R, Noolvi MN. Natural sources as potential anti-cancer agents: A review. *Int J Phytomedicine*. 2011;3(1):9–26.

45. Gordaliza M. Natural products as leads to anticancer drugs. *Clin Transl Oncol*. 2007;9(12):767–776.

46. Li Y, Ellis KL, Ali S, et al. Apoptosis-inducing effect of chemo-therapeutic agents is potentiated by soy isoflavone genistein, a natural inhibitor of NF-κB in BxPC-3 pancreatic cancer cell line. *Pancreas*. 2004;28(4):e90–e95.

47. Safarzadeh E, Sandoghchian Shotorbani S, Baradaran B. Herbal medicine as inducers of apoptosis in cancer treatment. *Adv Pharm Bull*. 2014;4(Suppl 1):421–427.

48. Pan M-H, Lai C-S, Wang H, Lo C-Y, Ho C-T, Li S. Black tea in chemo-prevention of cancer and other human diseases. *Food Sci Human Wellness*. 2013;2(1):12–21.

49. Hunter AM, LaCasse EC, Korneluk RG. The inhibitors of apoptosis (IAPs) as cancer targets. *Apoptosis*. 2007;12(9):1543–1568.

50. Bhakuni D, Gupta S. Alkaloids of *Litsea wightiana*. *Planta Med*. 1983;48(1):52–54.

51. Holloway DM, Scheinmann F. Co-occurrence of aporphine and biphenyl constituents in *Litsea turfosa*. *Phytochemistry*. 1973;12(6):1503–1505.

52. Yang JH, Li L, Wang YS, Zhao JF, Zhang HB, Luo SD. Two new aporphine alkaloids from *Litsea glutinosa*. *Helv Chim Acta*. 2005;88(9):2523–2526.

53. Rickard SE, Yuan YV, Chen J, Thompson LU. Dose effects of flaxseed and its lignan on N-methyl-N-nitrosourea-induced mammary tumorigenesis in rats. *Nutr Cancer*. 1999;35(1):50–57.

54. Shier WT. Mammalian cell culture on $5 a day: a laboratory manual of low cost methods. *Los Banos Univ Philippines*. 1991;64(8):9–16.

55. Ham Y-M, Yoon W-J, Park S-Y, et al. Quercitrin protects against oxidative stress-induced injury in lung fibroblast cells via up-regulation of Bcl-xL. *J Functional Foods*. 2012;4(1):253–262.

56. Mohan S, Abdul AB, Abdelwahab SI, et al. *Typhonium flagelliforme* induces apoptosis in CEMss cells via activation of caspase-9, PARP cleavage and cytochrome c release: its activation coupled with G0/G1 phase cell cycle arrest. *J Ethnopharmacol*. 2010;131(3):592–600.

57. Park H-S, Park K-I, Lee D-H, et al. Polyphenolic extract isolated from Korean *Lonicera japonica* Thunb. induce G2/M cell cycle arrest and apoptosis in HepG2 cells: involvements of PI3K/Akt and MAPKs. *Food Chem Toxicol*. 2012;50(7):2407–2416.

58. Pozo-Guisado E, Alvarez-Barrientos A, Mulero-Navarro S, Santiago-Josefat B, Fernandez-Salguero PM. The antiproliferative activity of resveratrol results in apoptosis in MCF-7 but not in MDA-MB-231 human breast cancer cells: cell-specific alteration of the cell cycle. *Biochem Pharmacol*. 2002;64(9):1375–1386.

59. Khan MA, Chen H-C, Wan X-X, et al. Regulatory effects of resveratrol on antioxidant enzymes: a mechanism of growth inhibition and apoptosis induction in cancer cells. *Mol Cells*. 2013;35(3):219–225.

60. Xiao D, Herman-Antosiewicz A, Antosiewicz J, et al. Diallyl trisulfide-induced G2–M phase cell cycle arrest in human prostate cancer cells is caused by reactive oxygen species-dependent destruction and hyper-phosphorylation of Cdc25C. *Oncogene*. 2005;24(41):6256–6268.

61. Olguín-Martínez M, Hernández-Espinosa DR, Hernández-Muñoz R. α-Tocopherol administration blocks adaptive changes in cell NADH/NAD+ redox state and mitochondrial function leading to inhibition of gastric mucosa cell proliferation in rats. *Free Radical Biol Med*. 2013;65: 1090–1100.

62. Rizzuto R, Giorgi C, Romagnoli A, Pinton P. Ca2+ signaling, mitochondria and cell death. *Curr Mol Med*. 2008;8(2):119–130.

63. Anatole PC, Guru SK, Bathelemy N, et al. Ethyl acetate fraction of *Garcina epunctata* induces apoptosis in human promyelocytic cells (HL-60) through the ROS generation and G0/G1 cell cycle arrest: a bioassay-guided approach. *Environ Toxicol Pharmacol*. 2013;36(3):865–874.

64. Vaux DL, Korsmeyer SJ. Cell death in development. *Cell*. 1999;96(2): 245–254.

65. Krajewski S, Krajewska M, Ellerby LM, et al. Release of caspase-9 from mitochondria during neuronal apoptosis and cerebral ischemia. *Proc Natl Acad Sci U S A*. 1999;96(10):5752–5757.

66. Susin SA, Lorenzo HK, Zamzami N, et al. Mitochondrial release of caspase-2 and -9 during the apoptotic process. *J Exp Med*. 1999;189(2): 381–394.

67. Li Z, Jo J, Jia J-M, et al. Caspase-3 activation via mitochondria is required for long-term depression and AMPA receptor internalization. *Cell*. 2010;141(5):859–871.

68. Green DR. At the gates of death. *Cancer Cell*. 2006;9(5):328–330.

69. Kluck RM, Bossy-Wetzel E, Green DR, Newmeyer DD. The release of cytochrome c from mitochondria: a primary site for Bcl-2 regulation of apoptosis. *Science*. 1997;275(5303):1132–1136.

70. Xiang J, Chao DT, Korsmeyer SJ. BAX-induced cell death may not require interleukin 1β-converting enzyme-like proteases. *Proc Natl Acad Sci U S A*. 1996;93(25):14559–14563.

71. Earnshaw WC, Martins LM, Kaufmann SH. Mammalian caspases: structure, activation, substrates, and functions during apoptosis. *Annu Rev Biochem*. 1999;68(1):383–424.

72. Gu Q, De Wang J, Xia HH, et al. Activation of the caspase-8/Bid and Bax pathways in aspirin-induced apoptosis in gastric cancer. *Carcinogenesis*. 2005;26(3):541–546.

73. Czabotar PE, Lessene G, Strasser A, Adams JM. Control of apoptosis by the BCL-2 protein family: implications for physiology and therapy. *Nat Rev Mol Cell Biol*. 2014;15(1):49–63.

74. Adams J, Cory S. The Bcl-2 apoptotic switch in cancer development and therapy. *Oncogene*. 2007;26(9):1324–1337.

75. Lee JS, Jung W-K, Jeong MH, Yoon TR, Kim HK. Sanguinarine induces apoptosis of HT-29 human colon cancer cells via the regulation of Bax/Bcl-2 ratio and caspase-9-dependent pathway. *Int J Toxicol*. 2012;31(1):70–77.

76. Zhu A, Zhou H, Xia J, et al. Ziyuglycoside II-induced apoptosis in human gastric carcinoma BGC-823 cells by regulating Bax/Bcl-2 expression and activating caspase-3 pathway. *Braz J Med Biol Res*. 2013; 46(8):670–675.

77. Ferenc P, Solár P, Kleban J, Mikeš J, Fedoročko P. Down-regulation of Bcl-2 and Akt induced by combination of photoactivated hypericin and genistein in human breast cancer cells. *J Photochem Photobiol B Biol*. 2010;98(1):25–34.

78. Zhang G-J, Kimijima I, Onda M, et al. Tamoxifen-induced apoptosis in breast cancer cells relates to down-regulation of bcl-2, but not bax and bcl-XL, without alteration of p53 protein levels. *Clin Cancer Res*. 1999; 5(10):2971–2977.

79. Mosser DD, Caron AW, Bourget L, et al. The chaperone function of hsp70 is required for protection against stress-induced apoptosis. *Mol Cell Biol*. 2000;20(19):7146–7159.

80. Jin S, Zhang Q, Kang X, Wang J, Zhao W. Daidzein induces MCF-7 breast cancer cell apoptosis via the mitochondrial pathway. *Ann Oncol*. 2010;21(2):263–268.

81. Naugler WE, Karin M. NF-κB and cancer – identifying targets and mechanisms. *Curr Opin Genet Dev*. 2008;18(1):19–26.

82. Verfaillie T, Garg AD, Agostinis P. Targeting ER stress induced apoptosis and inflammation in cancer. *Cancer Lett*. 2013;332(2):249–264.